Discontinuous Pulse Width Modulation in Flux Angle Control of Induction Motors

Mohammad Reza Mohebbi[1], Davood Arab Khaburi[1,*]

[1]Department of Electrical Engineering, Iran University of Science & Technology, Tehran, Iran

ARTICLE INFO	ABSTRACT
	In this study, flux angle control (FAC) with discontinuous modulation is presented for induction motor drives with the aim of optimizing motor and inverter losses under light load conditions. The proposed approach implements the discontinuous modulation technique in flux angle control for the first time and emphasizes proper drive performance while reducing its losses. The discontinuous pulse width modulation (DPWM) method optimizes switching by strategically injecting zero sequence voltages, reducing inverter losses and thermal stress on power electronics components, and improving system reliability. The proposed method is simulated in MATLAB software and compared with PWM and SVM techniques in drive efficiency and loss reduction. Comprehensive simulations confirm the superior performance of this combined approach and show the optimal balance between switching losses, harmonic quality, and current and torque ripple compared to PWM and SVM methods. The simplicity of implementation of the DPWM method, along with its ability to maintain acceptable output voltage quality and reduce overall system losses, while taking advantage of the advantages of PWM and SVM methods, emphasizes its suitability for practical industrial applications. This work contributes to the continued development of high-efficiency motor drive systems by highlighting the advantages of integrating flux angle control with discontinuous modulation strategies.

1. Introduction

Among the electro-mechanical devices transforming energy from electrical to mechanical, Induction Motor (IM) can be surely considered a workhorse of the industry when directly fed by the ac grid [1]. IMs are extensively utilized across various industrial sectors, including manufacturing, transportation, and energy systems, owing to their robustness, cost-effectiveness, and high efficiency. Notably, IMs account for more than 60% of industrial motor applications, consuming a significant portion of electrical energy in industries [2]. Consequently, enhancing the efficiency of these motors is a critical objective, aligning with global energy conservation goals and the increasing emphasis on sustainable practices.

Efficiency improvement strategies for IMs can be broadly categorized into two main approaches: structural modifications and advanced control techniques. Structural modifications involve optimizing the design of the rotor, stator, and winding configurations, which can be costly and complex to implement in existing systems. In contrast, control-based strategies offer a flexible and cost-effective solution by optimizing motor operation through intelligent control techniques, often referred to as Loss Minimization Algorithms (LMAs). These LMAs can be further classified into offline and online methods, with online methods subdivided into model-based, physics-based, and hybrid approaches [3].

One such advanced control method is Flux Angle Control (FAC), which aims to enhance motor efficiency, particularly under light-load conditions, by adjusting the angle between the stator current and the rotor flux direction. This method ensures optimal motor operation, minimizing losses by setting the flux angle to the

---

∗ Corresponding author
  E-mail address: khaburi@iust.ac.ir
  https://orcid.org/0000-0001-5861-0213

optimum value. A key component of flux angle control is the selection of an appropriate inverter modulation technique, which directly affects the quality of the motor current, the level of harmonic distortion, and the overall efficiency of the drive system.

Inverter modulation methods play a pivotal role in determining the performance of induction motor drives. Among the most commonly employed techniques are: Pulse Width Modulation (PWM), Space Vector Modulation (SVM) and Discontinuous Pulse Width Modulation (DPWM) are the most commonly employed techniques in the inverter modulation methods [4-6].

DPWM, in particular, has garnered significant attention due to its ability to achieve high efficiency by reducing switching losses. Various DPWM techniques have been proposed in the literature, including DPWM0, DPWM1, DPWM2, and DPWM3, each exhibiting unique characteristics and performance trade-offs. Recent studies indicate that DPWM can effectively reduce switching losses without significantly compromising output voltage quality or motor current THD [7].

The performance of each modulation method in the motor drives is evaluated based on key criteria, including Total Harmonic Distortion (THD) of the motor current, switching losses of the inverter, voltage quality at the inverter output, current ripple in the motor windings and torque ripple, which affects the smoothness of motor operation.

Mr Asiminoaei in [8] applies Discontinuous PWM in active power filters to reduce harmonics and improve power quality. It highlights lower switching losses and enhanced system efficiency. The method also improves filter performance and electromagnetic compatibility. [9] presents a generalized discontinuous PWM scheme for three-phase voltage source inverters. It optimizes switching patterns to reduce switching losses and improve inverter efficiency. The approach also ensures better control and lower harmonic distortion. In [10], the effects of continuous and discontinuous PWM schemes on power losses in voltage-source inverters for induction motor drives are compared. It analyzes how different modulation strategies impact switching and conduction losses. The findings guide optimal PWM selection to enhance drive efficiency. In [11], generalized continual-clamp and split-clamp PWM schemes are analyzed for induction motor drives. It discusses their effects on inverter losses, torque ripple, and harmonic performance. The study helps in choosing the best PWM strategy for efficient motor control. In [12], a new generalized method of discontinuous PWM strategies is proposed to minimize switching losses. It focuses on reducing inverter power losses while maintaining output performance.

This paper does not aim to reintroduce the concept of flux angle control (FAC), which was originally proposed by the authors [13, 14]. Instead, it investigates a novel aspect of FAC: its integration with discontinuous PWM (DPWM) and other modulation methods (like SVM and PWM). To the best of our knowledge, this is the first comparative analysis of FAC under different modulation schemes, highlighting its impact on losses, harmonic distortion, and real-time feasibility. The remainder of this paper is structured as follows: Section

2 presents a detailed explanation of the flux angle control method and its implementation. Section 3 provides an overview of the modulation techniques studied. Section 4 discusses the simulation setup and results, offering a detailed analysis of the performance of each modulation method. Finally, Section 5 concludes the study.

2. Flux Angle Control (FAC)

Given the importance of induction motors, as mentioned in the previous section, improving the efficiency of these motors has attracted significant attention from researchers. Consequently, various methods have been developed to reduce losses and enhance the overall efficiency of these motors. In general, the studies conducted in this area can be divided into two main categories: the first category involves studies focused on the optimal design of induction motor structures [15, 16], while the second category includes research on control strategies and optimal operation of these motors [17-20]. Flux angle control, which belongs to the second category, has recently been introduced to reduce motor losses at light load conditions [13, 14, 21]. The core idea of this control method lies in manipulating the angle between the stator current vector and the rotor flux vector (aligned along the d-axis). This angle, referred to as the flux angle (θ_s), significantly influences torque production and motor losses. According to the electromagnetic torque expression of an induction motor:

$$T = \frac{3}{2} \cdot \frac{p}{2} \cdot \frac{L_m}{L_r} |\vec{\lambda}_r| \cdot |\vec{I}_s| \cdot \sin(\theta_s) \qquad (1)$$

As shown in Fig. 1, increasing the flux angle while reducing the rotor flux magnitude allows the motor to produce the required torque while minimizing the magnetic field intensity, thus reducing both copper and core losses under light-load conditions.

Table I. List of Symbols

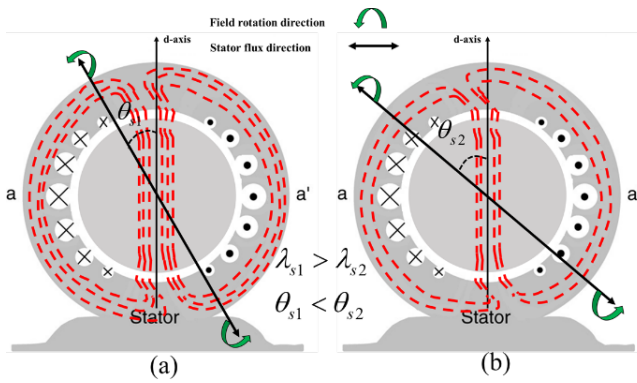| symbol	description	symbol	description
$R_s(\Omega)$	Stator resistance	p	Number of poles
$R_r(\Omega)$	Rotor resistance	$L_r(H)$	Rotor inductance
$R_{fe}(\Omega)$	Iron loss modeling resistor	$\vec{I}_s(A)$	Stator current vector
$L_m(H)$	Mutual inductance	$\vec{\lambda}_r(Web)$	Rotor flux vector
$L_{lr}(H)$	Rotor leakage inductance	$\theta_s(Deg)$	Rotor flux direction
ω_e	Rotating reference frame		

Fig. 1. Flux level and flux angle direction in rotor and stator in FAC

2.1. Minimization via Optimal Flux Angle

Total controllable losses in an induction motor can be expressed as the sum of stator copper loss, rotor copper loss, and iron loss. Assuming the rotor flux $\vec{\lambda}_r$ is aligned with the d-axis (i.e., $\lambda_{rq} = 0$), the optimal flux angle θ_s that minimizes total losses can be analytically derived. By taking the derivative of the total loss equation with respect to θ_s and setting it to zero, the optimal angle is found to be:

$$(\theta_s)_{opt} = a\tan(\frac{\beta.\sqrt{\gamma}+\alpha.\sqrt{\sigma}}{\sqrt{\alpha}-\alpha.\sqrt{\gamma}}) \qquad (2)$$

Where $\quad \alpha = \dfrac{\omega_e.L_m}{R_{fe}} \quad , \quad \gamma = R_s + \alpha^2.(R_s + R_{fe}) \quad,$

$\beta = 1 + \dfrac{L_m}{L_{lr}} \quad \sigma = R_r.(\dfrac{L_m}{L_{lr}})^2. + R_{fe}.\alpha^2 + R_s.(\alpha^2 + \beta^2)$

This equation determines the optimal flux angle that yields the **minimum total loss** for a given operating condition. Although the optimal flux angle depends on certain motor parameters, its sensitivity to variations in these parameters in minimal. The detailed derivation and parameter sensitivity analysis are provided in [13], and are not repeated here for brevity since the main focus of this work is on modulation strategy.

3. Overview of Modulation Techniques

Modulation techniques are essential for controlling the output of voltage source inverters (VSIs), which are widely used in electric motor drives, renewable energy systems, and power converters. These methods generate gate signals for power semiconductor switches in a way that allows the inverter to synthesize sinusoidal or quasi-sinusoidal AC output voltages from a DC source. The choice of modulation method significantly affects the harmonic quality of the inverter output, the efficiency of the system, the switching losses, and the thermal performance of the switching devices [2, 22]

In the context of flux angle control for induction motors, the role of modulation becomes even more critical. Since this control strategy adjusts the angle between stator current and rotor flux to minimize losses—particularly under light-load conditions—the performance and precision of the modulation directly influence the system's overall energy efficiency and dynamic response. Three major modulation approaches are considered in this study:

1. Sinusoidal Pulse Width Modulation (SPWM)
2. Space Vector Nodulation (SVM)
3. Discontinuous Pulse Width Modulation (DPWM)

Each method offers specific advantages and trade-offs in terms of voltage linearity, harmonic distortion, switching frequency behavior, and computational complexity.

3.1. Sinusoidal Pulse Width Modulation (SPWM)

Sinusoidal PWM is one of the earliest and most commonly used methods for inverter control. It involves comparing a sinusoidal reference signal with a triangular carrier waveform to generate switching signals. The main advantage of SPWM is its simplicity and ease of implementation. However, it suffers from limited voltage utilization and generates more switching events compared to more advanced techniques like SVM or DPWM [4].

If $V_{ref}(t)$ is the reference signal and the carrier is a triangle wave $V_{carrier}(t)$ then:

$$S(t) = \begin{cases} 1 & V_{ref}(t) > V_{carrier}(t) \\ 0 & otherwise \end{cases} \qquad (3)$$

This binary signal is then used to drive the inverter switches.

These methods suffer from limited DC bus utilization (approximately 78.5% of the DC voltage) and from a higher switching frequency, which results in increased switching losses.

3.2. Space Vector Nodulation (SVM)

Space Vector Modulation is a more advanced approach that considers the inverter switching states as vectors in the complex plane. SVM calculates the required output voltage vector and synthesizes it using a combination of the nearest active vectors and zero vectors within each switching period. This technique maximizes DC bus voltage utilization (up to 15% more than SPWM), offers lower total harmonic distortion (THD), and provides better control over switching transitions [5, 6].

Fig. 2 presents the eight inverter voltage vectors in conjunction with the reference voltage vector.
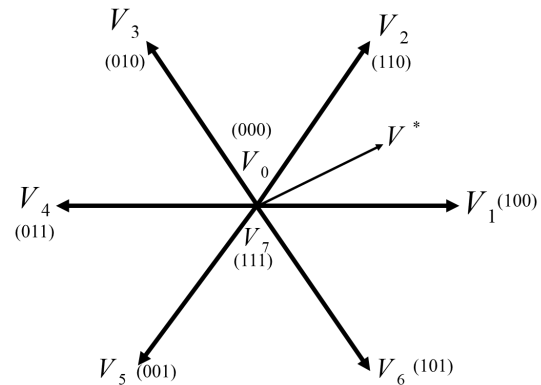

Fig. 2. Voltage vectors of all eight switching states along with the reference vector at SVM

Based on the angular position of the reference vector (i.e., the sector it lies in), the switching times are determined using the following equation, which is specifically applicable to angles between 0° and 60°.

$$V^* = d_1 V_1 + d_2 V_2 + \frac{d_0}{2} V_0 + \frac{d_0}{2} V_7 \qquad (4)$$

3.3. Discontinuous Pulse Width Modulation (DPWM)

Discontinuous PWM methods, such as DPWM0, DPWM1, and DPWM3, are designed to reduce switching losses by clamping one or more inverter legs to the positive or negative DC rail during portions of the switching cycle. By reducing the number of switching transitions per cycle, DPWM significantly lowers switching losses and improves thermal efficiency—particularly under high-frequency operation [7]. These methods are highly beneficial in flux angle control, where efficient switching becomes critical at low torque and low flux levels. However, DPWM may introduce additional harmonic components due to the discontinuities, requiring careful harmonic evaluation.

The core principle behind these techniques is to enhance performance by adding a zero-sequence component to the reference voltage vectors. Studies have demonstrated that the performance of a three-phase inverter improves when a suitable zero-sequence signal is added to the reference voltage waveform [17]. In all carrier-based PWM methods, the resulting reference signal can be represented as:

$$V^{**} = V^* + V_0 \qquad (5)$$

Where V^* is the reference signal and V_0 is the zero-sequence signal [23]. If the zero-sequence component is zero, the method is referred to as SPWM. However, when the added zero-sequence signal causes the phase legs to be clamped to either the positive or negative DC rail for part of each switching period, the method is known as DPWM. A block diagram illustrating the injection of the zero-sequence signal using a single common triangular carrier is shown in Fig. 3 [24].

There are six common implementations of Discontinuous PWM (DPWM) techniques. In all of these methods, each phase leg of a three-phase inverter remains unswitched (clamped) for 120° within each switching cycle. The methods differ in terms of the duration and positioning of the clamping intervals.
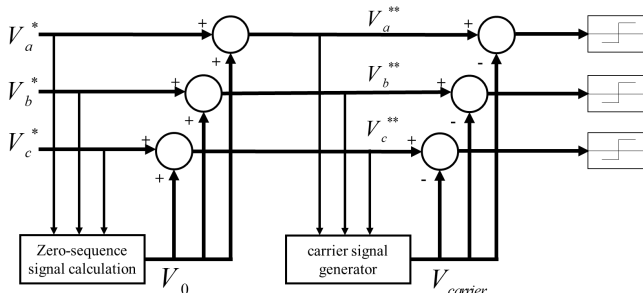
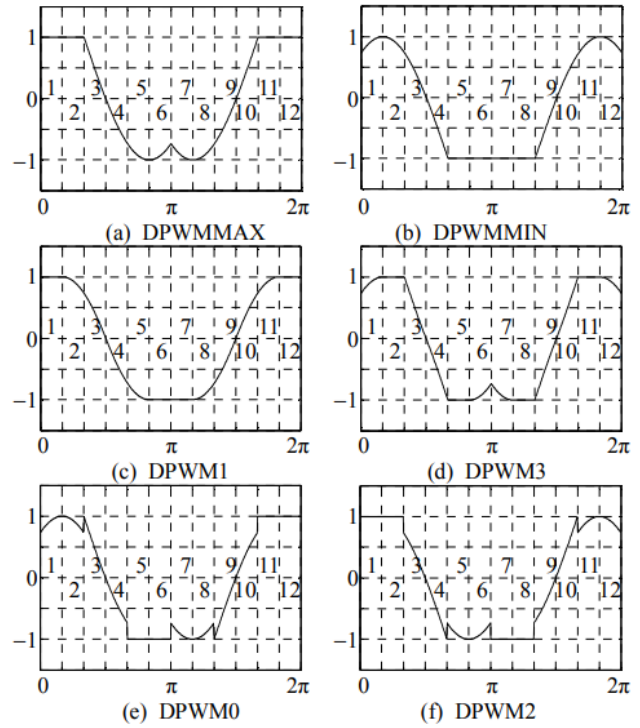**Fig. 3.** Block diagram of zero-sequence signal injection [25]

Fig. 4. Reference signal of common DPWM method [12]

In DPWM1, the 60° unmodulated (clamped) intervals are centered around both the positive and negative peaks of the fundamental reference voltage. This configuration performs best with resistive loads, where the peak current aligns with the peak voltage [3]. DPWM0 is the most suitable arrangement for capacitive loads, as its clamping period is centered 30° before the peak of the reference voltage. Conversely, DPWM2, with its clamping period centered 30° after the reference voltage peak, is best suited for inductive loads. The 60° clamping intervals can also be positioned anywhere between those used in DPWM0 and DPWM2. By aligning the clamping period as closely as possible with the peak current, switching losses can be minimized. DPWM3, on the other hand, features four 30° clamping intervals spaced 60° apart. Among the six DPWM strategies, DPWM3 yields the lowest harmonic distortion, whereas DPWM1 exhibit the highest [24].

In this paper, flux angle control is implemented using PWM, DPWM1, and SVM methods. In the DPWM1 method, the zero-sequence voltage is calculated according to Equation (6). Fig. 5 shows the normalized waveform of the reference voltage, zero-sequence voltage, and the modified reference voltage.

$$V_0 = \begin{cases} (-1 - V_b^*) & 0^0 \le \theta < 60^0 \\ (1 - V_a^*) & 60^0 \le \theta < 120^0 \\ (-1 - V_c^*) & 120^0 \le \theta < 180^0 \\ (1 - V_b^*) & 180^0 \le \theta < 240^0 \\ (-1 - V_a^*) & 240^0 \le \theta < 300^0 \\ (1 - V_c^*) & 300^0 \le \theta < 360^0 \end{cases} \qquad (6)$$
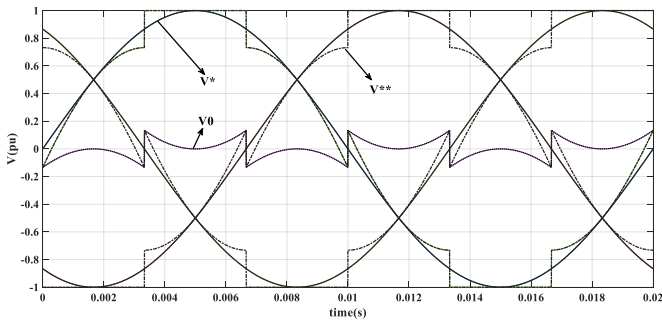
Fig. 5. DPWM1 modulation waveform

4. Simulation setup and results

In this section, the results of implementing the flux angle control method using SPWM, SVM, and DPWM modulation techniques in MATLAB software are examined. The characteristics of the induction motor used in the study are listed in Table **II**. Simulation results are provided for a load corresponding to 10% of the rated torque and 50% of the rated speed. Based on the motor parameters and Equation (2), the resulting flux angle is calculated to be approximately 45 degrees.

Table II. parameters of induction motor

Nominal rating of induction motor	
$P_n = 1.5\ Kw$	$R_s = 5.35\ \Omega$
$V_n = 220\ v$	$R_r = 3.15\ \Omega$
$I_n = 3.3\ A$	$L_{ls} = 11.33\ mH$
$\omega_n = 2860\ Rpm$	$L_{ls} = 11.33\ mH$
$T_n = 5\ N.m$	$L_m = 0.4941\ H$
$P = 2$	$R_{fe} = 2401\ \Omega$
$J = 0.0014\ kg.m^2$	$cos\ \varphi = 0.85$

The block diagram of flux angle control using the discontinuous modulation method is shown in Fig. 6. In this control strategy, the motor speed is first compared with the reference speed. The resulting error is processed by a PI controller to determine the reference torque. Based on the reference torque and the reference speed, and according to the motor parameters and Equation (2), the flux angle as well as the reference components of the stator current are calculated. By comparing the reference stator current components with the measured output

currents from the motor, the reference stator components are obtained. Finally, by transforming them into the three-phase system and calculating the zero-sequence voltage component, the reference three-phase voltages are determined. The PWM switching frequency is set to 10 kHz with a simulation step of 5 µs. The inner current loop is updated every switching period and designed for a bandwidth of 800 Hz (≈8% of 10 kHz), considering PWM and computational delays. The outer speed loop operates ten times slower, with a bandwidth of 80 Hz. PI controllers are tuned by pole-placement (symmetrical optimum) using motor electrical and mechanical parameters. The flux angle control and zero-sequence injection require only algebraic and trigonometric calculations. These operations are computationally lightweight compared with the 100-µs switching period, making real-time implementation feasible on standard ARM/DSP/FPGA hardware.[13].

Fig. 7 illustrates the motor's speed and torque output characteristics. This figure confirms that the motor is successfully achieving the required speed and torque. In this case (a), the flux angle is 45 degrees, while in vector control the flux angle is approximately 9 degrees. The flux magnitude in flux angle control is 0.5 Weber, compared to 1 Weber in vector control. The efficiency of flux angle control in this case is 24%, whereas in vector control it is approximately 10%. In section (b), the motor load change from 10% of rated torque and 50% of rated speed to 20% of rated torque and 40% of rated speed in the second 2 is plotted, which shows that the proposed method maintains its stability. Fig. 8 shows the current vector and flux angle in flux angle control and vector control at 10% of the rated torque and 50% of the rated speed. This figure clearly shows the increase in flux angle and the reduction in the motor's stator current. A reduction in stator current leads to a decrease in the flux level and consequently reduces motor losses.

In the following, we examine the quality of the inverter output voltage under flux angle control using three methods: SVM, PWM, and DPWM. To this end, we compare the inverter line voltage FFT, the phase current THD, the torque ripple, and the switching losses for these three methods
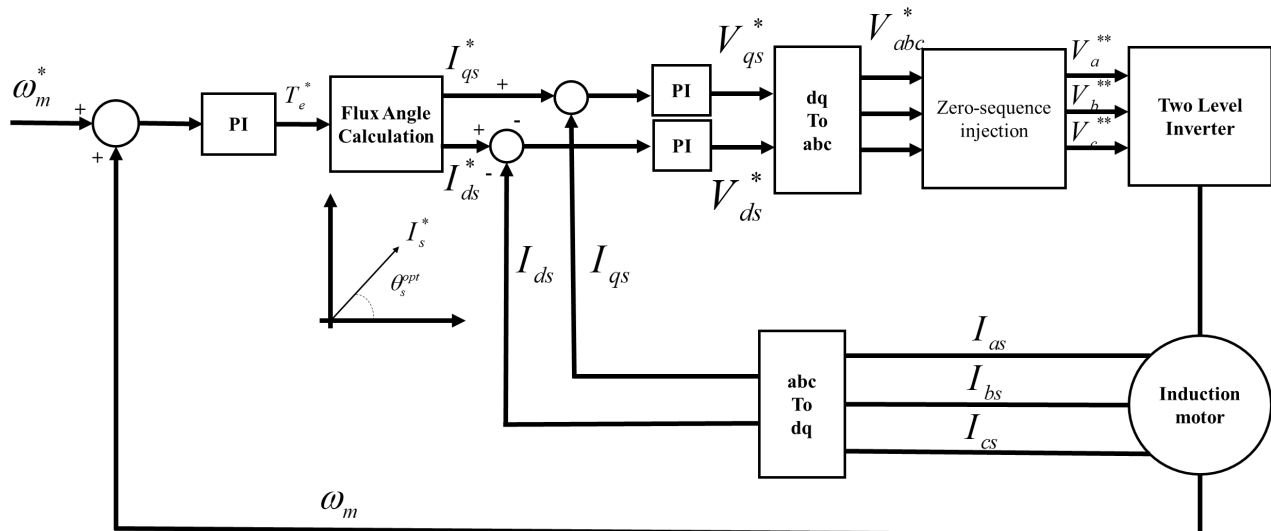

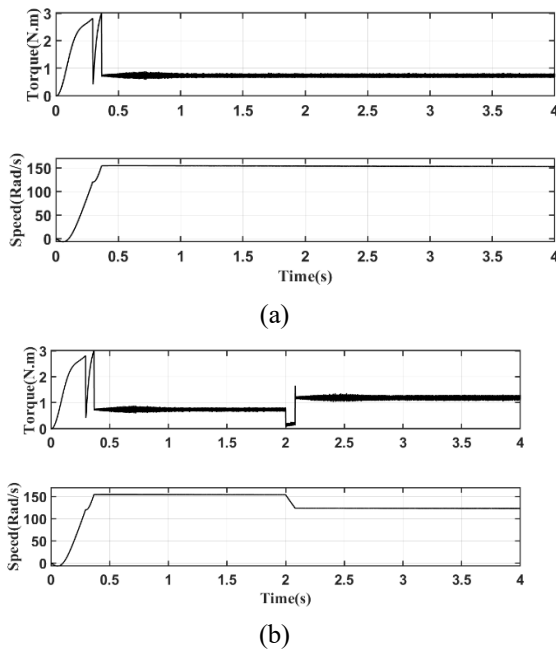**Fig. 6.** Block diagram of flux angle control with DPWM

(a)

(b)

Fig. 7. Torque and speed of motor in (a) 10% and 50% of rated Torque and speed and (b) 10% and 50% of rated Torque and speed to 20% and 40% of rated Torque and speed in
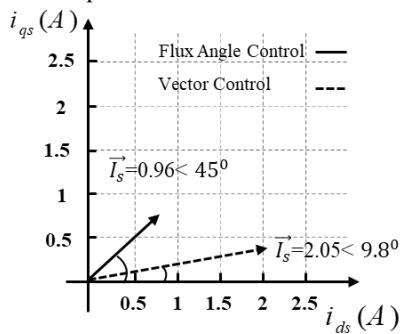

Fig. 8. Current Vector and flux angle in vector control and flux angle control in 10% of rated Torque and 50% of rated speed

Fig. 9 present the phase voltage waveforms for the three modulation methods. In the SVM method, the phase voltage waveform closely resembles a sinusoidal shape, oscillating between -200 V and 200 V (with a DC link voltage of 300 V). In contrast, the PWM and DPWM methods exhibit phase voltage waveforms oscillating between -150 V and 150 V.

Additionally, to better illustrate the periods when switching does not occur in the DPWM method, Fig. 10 compares the PWM and DPWM phase voltage waveforms. It can be seen that during certain intervals in the DPWM method, no switching events take place, effectively reducing switching losses.
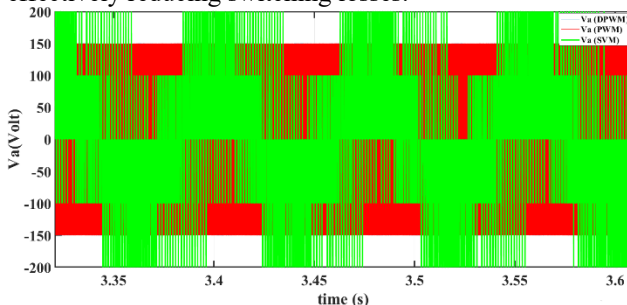

Fig. 9. Inverter output phase voltage for the three methods: SVM, PWM, and DPWM
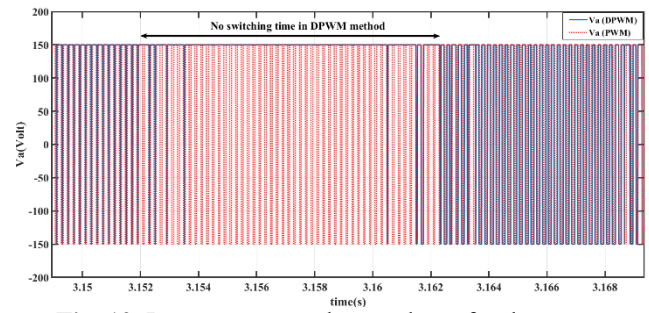

Fig. 10. Inverter output phase voltage for the two methods: PWM, and DPWM

Figures 11, 12, and 13 show the FFT of the inverter output line voltage for the three modulation methods: SVM, PWM, and DPWM1. The harmonic spectrum is obtained through FFT analysis of the simulated waveforms, with a sampling frequency of Fs=1/Ts, considering components up to the Nyquist limit.
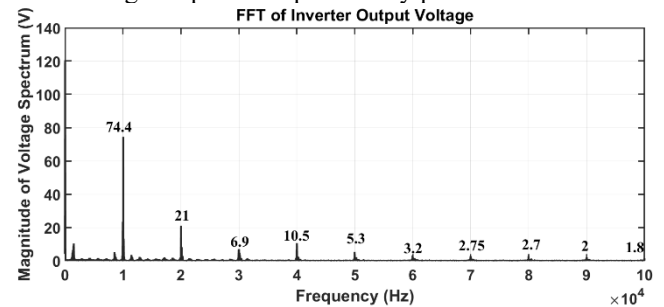

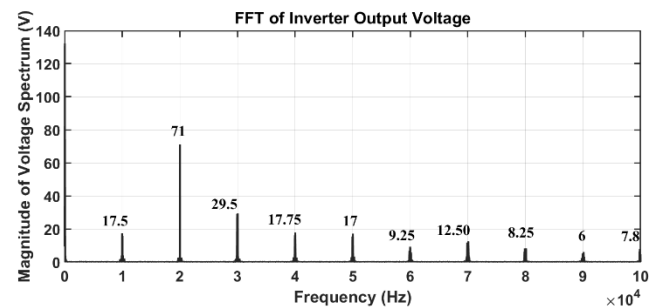**Fig. 11.** FFT of the inverter line output voltage in SVM

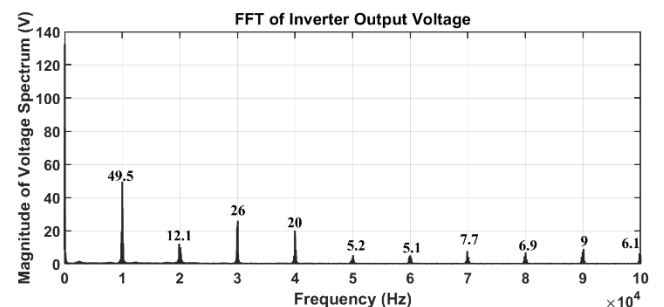**Fig. 12.** FFT of the inverter line output voltage in PWM

Fig. 13. FFT of the inverter line output voltage in DPWM

The analysis of the inverter output voltage spectra under the three modulation methods-SVM, PWM, and DPWM-reveals several important characteristics. The SVM technique produces a more uniform frequency spectrum, with lower amplitude of higher-order harmonics, indicating superior output voltage quality and reduced THD. This leads to improved motor performance and

reduced thermal losses. In contrast, the PWM method shows significant harmonic components at the switching frequency and its multiples. While it may have slightly higher harmonic content than SVM, PWM is easier to implement and control. The DPWM method demonstrates reduced switching frequency harmonics due to the clamping periods inherent in its operation. This effectively reduces switching losses, although the amplitude of some lower-order harmonics is slightly higher compared to SVM, which could impact dynamic performance. Overall, these observations highlight the trade-offs between output voltage quality and switching losses across the three modulation techniques.

Figures 14 and 15 show the phase current waveform and the motor output torque waveform, respectively. The phase current waveforms indicate that the current ripple is higher in the SVM method due to the reduced switching frequency. In contrast, the PWM and DPWM methods exhibit lower current ripple because of the higher switching frequency. The motor output torque, which directly depends on the phase current, shows a similar trend.
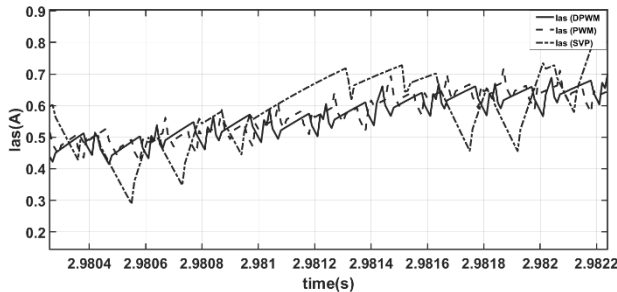

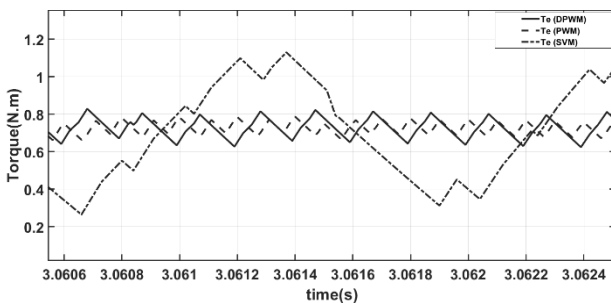**Fig. 14.** Motor phase current under SVM, PWM, and DPWM methods

Fig. 15. Output torque of the motor under SVM, PWM, and DPWM methods

Figures 16-18 respectively illustrate the stator current THD of the motor, the inverter line voltage, and inverter losses at 60% of the rated speed and 10–70% of the rated torque. The total harmonic distortion (THD) is calculated using MATLAB's built-in THD function, where the distortion is normalized with respect to the fundamental component and all higher-order harmonics up to the Nyquist frequency are included.

Under flux-angle control, the stator current THD obtained with DPWM is generally comparable to SVM and becomes the best option at 60% rated torque (–8.6 dB), whereas PWM—although exhibiting the cleanest line-voltage spectrum at low–medium loads (≤–60 dB)—shows pronounced degradation at high loads. The observed mid/high-load deterioration across all methods

is consistent with fixed PI gains tuned at 10% rated torque; gain scheduling or adaptive tuning would reduce ripple substantially. DPWM intentionally trades line-voltage THD for reduced switching activity and common-mode voltage, yet the machine inductance effectively filters high-frequency components so that the **current** THD remains low. Consequently, with proper controller scheduling, DPWM offers an attractive balance of current quality, efficiency, and EMI/CMV performance compared to SVM and PWM.
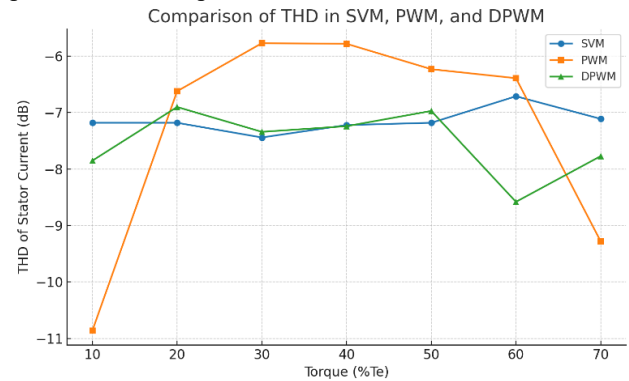

Fig. 16. Comparison of stator current THD (in dB) for SVM, PWM, and DPWM under different torque levels
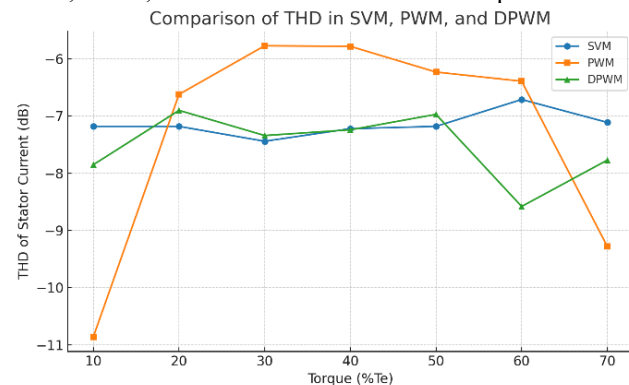

Fig. 17. Comparison of line voltage THD (in dB) for SVM, PWM, and DPWM under different torque levels
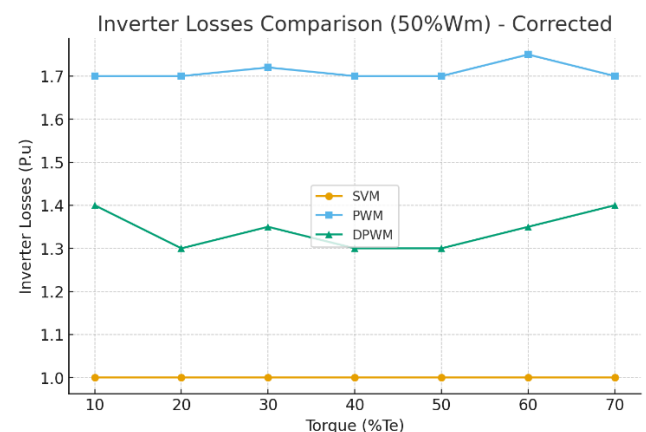

Fig. 18. Comparison of inverter losses for SVM, PWM, and DPWM

5. Conclusion

In This paper presented flux angle control combined with DPWM for induction motor drives. Compared with PWM and SVM, the DPWM method reduces switching losses by about 30%, directly improving efficiency and reliability. While PWM achieves the lowest line-voltage

THD and SVM provides stable but higher current distortion, DPWM offers a balanced compromise: it maintains current THD at levels comparable to SVM—even outperforming it at certain loads—while accepting higher voltage THD that is naturally filtered by the motor inductance. Overall, DPWM provides an efficient, practical, and reliable modulation strategy with acceptable waveform quality.

6. References

1. Di Nardo, M., et al., *Rotor slot design of squirrel cage induction motors with improved rated efficiency and starting capability.* IEEE Transactions on Industry Applications, 2022. **58**(3): p. 3383-3393.

2. Holmes, D.G. and T.A. Lipo, *Pulse width modulation for power converters: principles and practice.* 2003: John Wiley & Sons.

3. Jung, C., C.R.C. Torrico, and E.G. Carati, *Adaptive loss model control for robustness and efficiency improvement of induction motor drives.* IEEE Transactions on Industrial Electronics, 2021. **69**(11): p. 10893-10903.

4. Pramod, P., *Inverter Pulse Width Modulation Control Techniques for Electric Motor Drive Systems.* arXiv preprint arXiv:2310.03362, 2023.

5. Kirankumar, B., Y. Siva Reddy, and M. Vijayakumar, *Multilevel inverter with space vector modulation: intelligence direct torque control of induction motor.* IET power electronics, 2017. **10**(10): p. 1129-1137.

6. Trzynadlowski, A.M., *Introduction to modern power electronics.* 2015: John Wiley & Sons.

7. Ruiz-González, A., et al., *Discontinuous PWM strategy with frequency modulation for vibration reduction in asynchronous machines.* Machines, 2023. **11**(7): p. 705.

8. Asiminoaei, L., P. Rodriguez, and F. Blaabjerg, *Application of discontinuous PWMModulation in active power filters.* IEEE Transactions on Power Electronics, 2008. **23**(4): p. 1692-1706.

9. Ojo, O. and P. Kshirsagar. *The generalized discontinuous PWM modulation scheme for three-phase voltage source inverters.* in *IECON'03. 29th Annual Conference of the IEEE Industrial Electronics Society (IEEE Cat. No. 03CH37468).* 2003. IEEE.

10. Wu, Y., et al., *Comparison of the effects of continuous and discontinuous PWM schemes on power losses of voltage-sourced inverters for induction motor drives.* IEEE Transactions on Power Electronics, 2010. **26**(1): p. 182-191.

11. Das, S., et al., *Analysis of generalized continual-clamp and split-clamp PWM schemes for induction motor drive.* Sādhanā, 2019. **44**(2): p. 36.

12. An, S., et al. *Research on a new and generalized method of discontinuous PWM strategies to minimize the switching loss.* in *IEEE PES Innovative Smart Grid Technologies.* 2012. IEEE.

13. Mohebbi, M.R. and D. Arab Khaburi, *Robust flux angle control of induction motors to improve efficiency at light loads.* IET Electric Power Applications, 2024.

14. Mohebbi, M.R., D. Arab Khaburi, and M. Khosravi, *Flux Angle Control to Improve the Efficiency of Induction Motors.* TABRIZ JOURNAL OF ELECTRICAL ENGINEERING, 2021. **50**(4): p. 1785-1795.

15. Alberti, L. and D. Troncon, *Design of electric motors and power drive systems according to efficiency standards.* IEEE Transactions on Industrial Electronics, 2020. **68**(10): p. 9287-9296.

16. Li, J., C. Di, and X. Bao, *Efficiency improvement for submersible motors by optimizing the ratio of diameter to shaft length.* IEEE Transactions on Magnetics, 2021. **58**(2): p. 1-6.

17. Pugachev, A. and A. Kosmodamianskiy. *Induction motor scalar control system with power losses minimization.* in *2019 International Conference on Industrial Engineering, Applications and Manufacturing (ICIEAM).* 2019. IEEE.

18. Nandy, S., S. Das, and A. Pal. *Online golden section method based loss minimization scheme for direct torque controlled induction motor drive.* in *2018 8th IEEE India International Conference on Power Electronics (IICPE).* 2018. IEEE.

19. Bizhani, H., et al. *Comparative analysis of search algorithm based loss minimization techniques used in vector controlled induction motors.* in *2020 2nd International Conference on Smart Power & Internet Energy Systems (SPIES).* 2020. IEEE.

20. Olajube, A. and O.M. Anubi. *Model-based Loss Minimization Control of a Squirrel cage Induction Motor Drive with shorted Rotor under Indirect Field Orientation.* in *2023 IEEE Conference on Control Technology and Applications (CCTA).* 2023. IEEE.

21. Mohebbi, M., et al. *Predictive control of flux angle for induction motors.* in *2019 IEEE International Symposium on Predictive Control of Electrical Drives and Power Electronics (PRECEDE).* 2019. IEEE.

22. Van Der Broeck, H.W., H.-C. Skudelny, and G.V. Stanke, *Analysis and realization of a pulsewidth modulator based on voltage space vectors.* IEEE transactions on industry applications, 1988. **24**(1): p. 142-150.

23. Yuan, X., Y. Li, and C. Wang, *Objective optimisation for multilevel neutral-point-clamped converters with zero-sequence signal control.* IET Power Electronics, 2010. **3**(5): p. 755-763.

24. Kujala, J., *DISCONTINUOUS PWM TECHNIQUES IN THREE-PHASE POWER CONVERTERS.* 2020.

25. Hava, A.M. and N.O. Cetin, *A generalized scalar PWM approach with easy implementation features for three-phase, three-wire voltage-source inverters.* IEEE Transactions on Power Electronics, 2010. **26**(5): p. 1385-1395.